Individual Ionization Constants of All the Carboxyl Groups in Ribonuclease HI from *Escherichia coli* Determined by NMR

Yasushi Oda,[‡,§] Toshio Yamazaki,[∥,⊥] Kuniaki Nagayama,[∥,#] Shigenori Kanaya,[‡] Yutaka Kuroda,[‡] and Haruki Nakamura*[,‡]

Protein Engineering Research Institute, 6-2-3 Furuedai, Suita, Osaka 565, Japan, and Biometrology Lab, JEOL Ltd., Musashino, Akishima, Tokyo 196, Japan

Received November 22, 1993; Revised Manuscript Received February 14, 1994[⊗]

ABSTRACT: All of the individual carboxyl groups (the side-chain carboxyl groups of Asp and Glu, and the C-terminal α-carboxyl group) in *Escherichia coli* ribonuclease HI, which is an enzyme that cleaves the RNA strand of a RNA/DNA hybrid, were pH-titrated, and their ionization constants (pK_a) were determined from an analysis of the pH-dependent chemical shifts of the carboxyl carbon resonances obtained from ^1H–^{13}C heteronuclear two-dimensional NMR. The pK_a values in the enzyme varied widely among individual residues, for example, in the unusual pK_a values for two important catalytic residues, Asp10 (pK_a 6.1) and Asp70 (pK_a 2.6). Moreover, remarkable two-step titrations were observed for these carboxylates. The binding of Mg^{2+} ion to the enzyme, which is the cofactor necessary for catalytic activity, caused no significant change in the pK_a values of the carboxyl groups, except for that of Asp10. The variations of the pK_as that were dependent on the microenvironment in the protein were theoretically reproduced to compare with the experimental results by a numerical calculation, using a continuum electrostatic model. Most of the significant pK_a decreases were brought about through strong electrostatic interactions with the neighboring basic amino acids, Arg or Lys. The pK_a shifts and the two-step titrations of Asp10 and -70, which are close to each other, were interpreted to be due to the neighboring effect of two functional groups, as observed in the interacting titratable groups of a dicarboxyl compound or in the active site carboxylates of lysozyme and aspartic protease. The role of Asp10 in the catalytic action is either to be the proton donor to the RNA moiety or the binding partner of the Mg^{2+} ion cofactor. Asp70, on the other hand, is considered to be the proton acceptor from a water molecule.

Ribonuclease H (RNase H)[1] (EC 3.1.26.4) is an endonuclease that specifically cleaves the RNA strand of a DNA/RNA hybrid. It requires a divalent cation, such as Mg^{2+} or Mn^{2+}, as a cofactor for the enzymatic reaction (Crouch & Dirksen, 1982). The importance of this enzyme is evidenced by its wide presence in living systems, ranging from *Escherichia coli* to human (Crouch & Dirksen, 1982), although its physiological role in metabolism is still unclear. It is also present in retroviruses and is found in human immunodeficiency virus (HIV) as one of the domains in the reverse transcriptase (Wintersberger, 1990). Structural analyses by crystallography have shown that the three-dimensional structure of the RNase H domain in HIV-1 reverse transcriptase (Davies *et al.*, 1991; Arnold *et al.*, 1992; Kohlstaedt *et al.*, 1992) is similar to that of RNase HI from *E. coli* (Katayanagi *et al.*, 1990; Yang *et al.*, 1990) and to that of the RNase H from *Thermus thermophilus* (Ishikawa *et al.*, 1993).

Among the various RNase H proteins, *E. coli* RNase HI has been most extensively studied for its structure–function relationship by various techniques, including X-ray analysis (Katayanagi *et al.*, 1990, 1992; Yang *et al.*, 1990), site-directed mutagenesis (Crouch, 1990; Kanaya *et al.*, 1990, 1991a–c), and nuclear magnetic resonance (NMR) studies (Nagayama *et al.*, 1990; Yamazaki *et al.*, 1991, 1993; Nakamura *et al.*, 1991; Oda *et al.*, 1991, 1992, 1993). The enzyme is composed of a single polypeptide chain of 155 amino acid residues (Kanaya & Crouch, 1983) with an isoelectric point (p*I*) of 9.0 (Kanaya *et al.*, 1989). On the basis of a series of investigations, three amino acid residues with carboxyl groups (Asp10, Glu48, and Asp70) are postulated to form the catalytic site of the enzyme. These three residues are fully conserved in RNases H extracted from various species (Doolittle *et al.*, 1989).

Two alternative mechanisms have been proposed for the catalytic function of the enzyme. One is a two-metal-ion mechanism (Yang *et al.*, 1990), in which the water molecule that will hydrolyze the phosphodiester bond is activated by the metal ion bound to the catalytic residues, Asp10, Glu48, Asp70, and Asp134. The other is a carboxylate–hydroxyl relay mechanism (Nakamura *et al.*, 1991), in which the water molecule is activated by one of the three carboxylates of the catalytic residues, Asp10, Glu48, and Asp70. The finding that Mn^{2+} binds at two sites in the RNase H domain of HIV reverse transcriptase supports the two-metal-ion mechanism (Davies *et al.*, 1991). In contrast, the identification of a single metal binding site in the substrate-free enzyme by X-ray crystallographic analyses (Katayanagi *et al.*, 1990, 1992) and an NMR study (Oda *et al.*, 1991) supports the carboxylate–hydroxyl relay mechanism. The carboxylate–hydroxyl relay mechanism is also supported by a study using inert transition-metal complexes as probes (Jou & Cowan, 1991). To reveal the catalytic mechanism of the enzyme, the ionization states of the carboxyl groups involved in the catalytic action have

* To whom correspondence should be addressed.
‡ Protein Engineering Research Institute.
§ Present address: Tokyo Research Laboratories, Kyowa Hakko Kogyo Co. Ltd., Machida, Tokyo 194, Japan.
∥ JEOL Ltd.
⊥ Present address: Department of Medical Genetics, University of Toronto, Toronto, Ontario, Canada.
Present address: Department of Pure and Applied Sciences, The University of Tokyo, Komaba, Meguro-ku, Tokyo 153, Japan.
⊗ Abstract published in *Advance ACS Abstracts,* April 1, 1994.
[1] Abbreviations: HIV, human immunodeficiency virus; HSQC, heteronuclear single-quantum coherence; RNase H, ribonuclease H.

0006-2960/94/0433-5275$04.50/0

to be known. This was our motivation to pursue a comprehensive study to determine all the pK_a values of the carboxyl groups in the enzyme.

NMR provides a powerful method to determine the pK_a values of ionizable groups from the chemical shift variation (Jardetzky & Roberts, 1981). The pK_a values for the carboxyl groups (the side-chain carboxyl groups of Asp and Glu, and the C-terminal α-carboxyl group) are obtained by analyzing the curves of pH titrations of carboxyl groups, which are directly observed by carboxyl carbons with ^{13}C NMR or indirectly observed by protons adjacent to the carboxyl groups with ^1H NMR. Experiments to determine the individual pK_a values of all the carboxyl groups in a protein have been reported for basic pancreatic trypsin inhibitor (BPTI, 58 residues) using one-dimensional (1D) ^1H and ^{13}C NMR techniques (Richarz & Wüthrich, 1978) and mouse epidermal growth factor (EGF, 53 residues) using two-dimensional (2D) ^1H NMR techniques (Kohda *et al.*, 1991). In the present study, we used a ^1H–^{13}C heteronuclear 2D NMR technique, $^{13}C'$–(^{13}C)–^1H HSQC/HSQC (Yamazaki *et al.*, 1993), to observe the carboxyl carbon and the adjacent proton resonances simultaneously. The cross peaks of the carboxyl groups in the 2D spectrum have already been assigned at pH 5.5 using heteronuclear three-dimensional NMR techniques (Yamazaki *et al.*, 1993). On the basis of the results, the pH-dependent chemical shifts of the resonances for the individual carboxyl groups were traced.

There are some complications in the interpretation of the observed titration curves, because the charge state of the ionizable groups in proteins is governed not only by the intrinsic acidity of the group but also by other factors, such as electrostatic interactions from neighboring ionizable groups and the heterogeneous dielectric environment in the protein solution system. It is, therefore, important to reproduce the pK_a by numerical calculations to identify the individual pK_a of the concerned group. Various models to evaluate electrostatic effects in proteins have been proposed (Linderstrøm-Lang, 1924; Tanford & Roxby, 1972; Bashford & Karplus, 1990; Bashford & Gerwert, 1992; Bashford *et al.*, 1993; Yang *et al.*, 1993). In the present study, we used the complete statistical mechanical method (Bashford & Karplus, 1990; Bashford *et al.*, 1992), which provides a stable result, even for a system with strongly interacting sites (Yang *et al.*, 1993).

On the basis of the individual pK_a values of all the carboxyl groups in *E. coli* RNase HI, the relationship between the observed pK_a values and the tertiary structure of the enzyme is discussed. The catalytic mechanism of *E. coli* RNase HI is then considered.

MATERIALS AND METHODS

Sample Preparation. The preparation and purification of *E. coli* RNase HI were as described previously (Nakamura *et al.*, 1991). To uniformly label the enzyme with ^{13}C, *E. coli* strain JM109, in which plasmid pJAL600 (Kanaya *et al.*, 1993) was transformed, was grown in M9 minimum culture medium including [$^{13}C_6$]glucose (98 atom %; Shoko Co., Ltd., Tokyo) as the sole carbon source (1.5 g/L of culture). All the NMR samples were prepared by dissolving the uniformly ^{13}C-labeled enzyme in 99.9% ^2H_2O containing 0.1 M NaCl. A total of 0.3 mL of each sample was stored in 5-mm NMR microtubes (BMS005, Shigemi Standard Joint Ind. Co., Ltd., Tokyo) (Takahashi & Nagayama, 1988).

NMR Spectroscopy. All the NMR experiments were carried out at 27 °C with an AM-500 spectrometer (Bruker), using frequencies of 500 MHz for the ^1H spin and 125 MHz for the ^{13}C spin. Proton and carbon chemical shifts were calibrated from the shift standards of sodium 3-trimethylsilylpropionate (TSP) and tetramethylsilane (TMS), respectively.

The pulse sequence for the 2D $^{13}C'$–(^{13}C)–^1H HSQC/HSQC experiment has been described previously (Yamazaki *et al.*, 1993). The residual water resonance was suppressed by preirradiation. The observation center was set at 4.78 ppm for ^1H and 40 ppm for ^{13}C. The spectral width of ω_1 (^{13}C resonances) was 3800 Hz, and ω_2 (^1H resonances) was 6000 Hz. The 2D NMR spectra were acquired with 1024 increments in the t_1 direction and 1024 data points in the t_2 direction. A total of 16–48 scans was accumulated for each t_1 increment, with a 1.0-s relaxation delay. The accumulation time of the time domain signals was 8.5–20.5 h. The time domain data were zero-filled to 4096 in the t_1 dimension and to 2048 in the t_2 dimension before Fourier transformation.

pH Titration Experiment. The chemical shifts of the CO carbons and the adjacent CH proton resonances for the side chains of Asp, Glu, Asn, and Gln and the main-chain carbonyls were observed by the 2D $^{13}C'$–(^{13}C)–^1H HSQC/HSQC under various pH conditions. It is worth noting that a sharp decrease in the solubility of the protein occurred at pH values above 6.5, especially near the isoelectric point (pI 9.0). Furthermore, the protein was precipitated by the addition of NaO^2H to adjust the pH of the sample solution. Therefore, we had to prepare two types of NMR samples for the pH titration experiment: one was the 1.5 mM enzyme solution pH-adjusted at 5.5–6.0, which was concentrated by ultrafiltration, and the other was the 0.7 mM solution at pH 7.8, which was prepared by dissolving the lyophilized enzyme in ^2H_2O containing 0.1 M NaCl at pH 8. The pH titration experiment for the metal ion-free enzyme was initiated at either pH 6.0 or 7.8, and then the pH was progressively decreased by the addition of ^2HCl to 2.0 or 5.5, respectively. The pH titration in the presence of 150 mM $MgCl_2$ was done in the range from 5.5 to 2.5. The protein was precipitated below a pH of 2.5 in the presence of 150 mM $MgCl_2$. The pH values reported here were not corrected for isotope effects.

Mg^{2+} Titration Experiment. The chemical shift changes that appeared to follow the addition of $MgCl_2$ were observed using the 2D $^{13}C'$–(^{13}C)–^1H HSQC/HSQC. The concentration of the enzyme was 1.5 mM, and that of $MgCl_2$ was 1.5–150 mM, dissolved in ^2H_2O containing 0.1 M NaCl at a pH of 5.5. The NMR sample titrated by 150 mM $MgCl_2$ was also used for the pH titration experiment.

Analysis of pH Titration Curves. The pK_a values were obtained by a nonlinear least-squares fit of the titration curves to the theoretical titration curves (Shrager *et al.*, 1972). The p$K_a^{1/2}$, which is the pH where the carboxyl group is half-protonated, was determined from the fitted curves. In this report, the p$K_a^{1/2}$ of each carboxyl group obtained from the ^{13}C data is considered to be the intrinsic pK_a for the discussion of the ionization of the carboxyl groups. On the other hand, the pK_a^{app} values, defined as the apparent macroscopic ionization constants by Shrager *et al.* (1972), were also calculated for the two-step titration curves of the CO carbons of Asp10 and Asp70 and the complicated curves of the CH protons of the adjacent residues.

Theoretical Calculation of the pK_a Value for Each Carboxyl Group. In order to interpret the multistep titration curves, a macroscopic dielectric model was employed. First, the electrostatic interaction energies were numerically calculated by solving the Poisson–Boltzman equations, using a highly vectorized computer program developed by Nakamura and

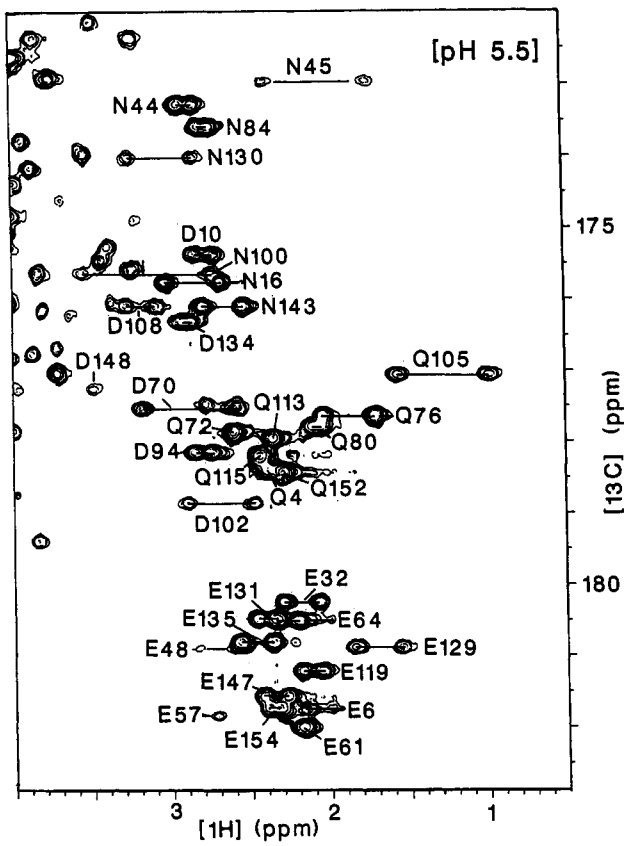

FIGURE 1: Expanded 2D $^{13}C'$–(^{13}C)–^{1}H HSQC/HSQC spectrum for the region of the cross peaks between the side-chain carbonyls and the carboxyl carbons (the $C^{\gamma}O$ carbons of Asp and Asn, and the $C^{\delta}O$ carbons of Glu and Gln) and the adjacent protons (the $C^{\beta}H$ protons of Asp and Asn, and the $C^{\gamma}H$ protons of Glu and Gln) of the uniformly ^{13}C-labeled *E. coli* RNase HI at 27 °C in $^{2}H_2O$ containing 0.1 M NaCl, at pH 5.5. The protein concentration was 1.5 mM.

Nishida (1987). It is based upon the algorithm of Warwicker and Watson (1982) and includes corrections of the error due to the finite boundary effect. From the coordinates of the crystal structure of *E. coli* RNase HI (Katayanagi *et al.*, 1992), a brick model for the protein–solvent system was built, composed of a 70 × 80 × 60 Å^3 rectangle with a 1.0-Å lattice spacing. Since we focused on the ionization of the carboxyl groups, a very simple charge distribution was assumed: for Arg and Lys side chains, +e was set on the Nζ and Cζ atoms, respectively. For His side chains, except His114, which is always neutral, the averaged charges calculated with the experimental pK_a values (Oda *et al.*, 1993) were set on the mean positions of the Nδ1 and Nε2 atoms for each pH condition. The backbone peptide groups were assumed to have partial charges to reflect the local dipole moment, 3.46 D (Hol *et al.*, 1978): N, –0.2e; HN, +0.2e; C, +0.42e; and O, –0.42e. The N-terminus was assumed to have +e throughout the pH region investigated. For the ionized carboxyl groups of the Asp and Glu side chains and the C-terminus, –0.5e was assigned to each oxygen atom. For the neutral carboxyl groups, no charges were assigned. To improve the spatial resolution for the discrete brick model, the particle–particle/particle–mesh algorithm (Nakamura, 1988) was employed. The dielectric constants, both in the solvent (ϵ_s) and in the border region (ϵ_b) with 1.4-Å width, were fixed at 77.6, and the dielectric constant in the interior of the protein (ϵ_p) was set to either 4 or 10 (Sakamoto *et al.*, 1989). The Poisson–Boltzmann equation was linearized in the solvent region with an ionic strength of 0.1 M.

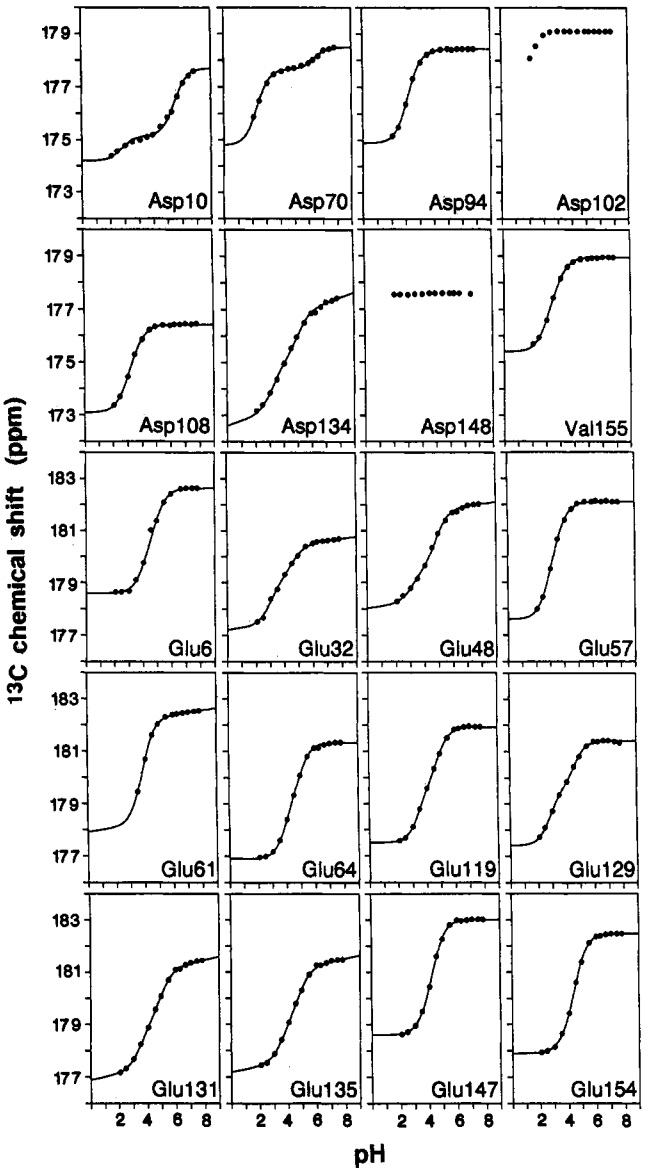

FIGURE 2: pH dependence of the chemical shifts of the carboxyl carbon resonances for all of the carboxyl groups in *E. coli* RNase HI. The pH titration experiments were carried out by measuring the 2D $^{13}C'$–(^{13}C)–^{1}H HSQC/HSQC spectra at different pH values in $^{2}H_2O$ containing 0.1 M NaCl at 27 °C. The fitted titration curves are also shown by solid lines.

Next, using the framework developed by Bashford and Karplus (1990) and by Yang *et al.* (1993), the degree of ionization of each carboxyl group was calculated directly from the partition function of the system by taking a Boltzmann weighted sum over all possible protonation states at each pH. Any protonation state of this system is defined as the combination of the state of each carboxyl site, according to whether each site is protonated or unprotontated. From the individual curves of the degree of ionization, the associated p$K_a^{1/2}$ of all the carboxyl groups and the pK_a^{app} for Asp10 were also determined in the same manner as for the experimental titration curves.

RESULTS

Determination of the pK_a Values of Carboxyl Groups. An expanded $^{13}C'$–(^{13}C)–^{1}H HSQC/HSQC spectrum of the uniformly ^{13}C-labeled *E. coli* RNase HI at pH 5.5, in the solution containing 0.1 M NaCl at 27 °C, is shown in Figure 1. The $^{13}C'$–(^{13}C)–^{1}H HSQC/HSQC experiments have shown

Table 1: Observed Ionization Constants (pK_a), with and without the Mg^{2+} Ion, of Carboxyl Groups in *E. coli* RNase HI at 27 °C for the Sample Solution Containing 0.1 M NaCl

	Mg^{2+}-free enzyme $pK_a^{1/2}$ [a]			Mg^{2+}-bound enzyme	
residue	^{13}C	^1H_a	^1H_b	$pK_a^{1/2}$ [b] ^{13}C	$\Delta\delta$ (ppm)[c]
Asp10	6.1 (6.5/2.8)	4.6 (6.5/3.7)	5.3 (6.2/3.1)	4.2 (4.7/1.8)	1.68
Asp70	2.6 (6.4/2.3)	5.6 (5.9/2.9)	2.7 (6.7/2.6)	3.4 (4.6/2.7)	1.02
Asp94	3.2	3.3	3.4	3.4	0.06
Asp102	<2	ND	ND	<2	0.00
Asp108	3.2	4.0	3.8	3.5	−0.03
Asp134	4.1	4.1	4.2	4.2	0.60
Asp148	<2	ND	ND	<2	−0.06
Asp(normal)	4.0[d]				
Glu6	4.5	ND	3.3	4.5	0.09
Glu32	3.6	3.4	3.4	4.0	0.12
Glu48	4.4	4.3	3.7	4.4	0.30
Glu57	3.2	4.6	ND	3.4	0.00
Glu61	3.9	4.3		4.0	0.00
Glu64	4.4	ND	4.6	4.5	0.06
Glu119	4.1	5.4	4.3	4.3	0.24
Glu129	3.6	3.3	4.3	4.0	0.12
Glu131	4.3	4.3	5.0	4.4	0.33
Glu135	4.3	4.9	4.5	4.3	0.33
Glu147	4.2	4.3	4.2	4.2	0.15
Glu154	4.4	4.2	4.4	4.4	0.18
Glu(normal)	4.5[d]				
Val155	3.4[e]	3.3		3.5	−0.09
α-COOH(normal)	3.6[d]				

[a] The experimental $pK_a^{1/2}$ values in the absence of $MgCl_2$. The $pK_a^{1/2}$ is defined as the pH where the ionized group is half protonated, as determined from curve fitting. The number in parentheses refers to the pK_a^{app} values, defined as the apparent macroscopic ionization constants by Shrager *et al.* (1972). [b] The experimental $pK_a^{1/2}$ values in the presence of 150 mM (100 equiv) to the enzyme) $MgCl_2$. [c] The ^{13}C chemical shift difference ($\Delta\delta$) of the carboxyl carbon resonances in the absence (a) and in the presence of 150 mM $MgCl_2$ (b) at pH 5.5, defined as $\Delta\delta = \delta(b) - \delta(a)$. [d] The normal pK_a value in the absence of any interactions. Data taken from Fersht (1985). [e] The experimental $pK_a^{1/2}$ value of the C-terminal α-COOH group.

a correlation between the CO carbon resonance and the adjacent CH proton resonance. We can observe the cross peaks between the side-chain carbonyl and the carboxyl carbon resonances (the $C^{\gamma}O$ carbons of Asp and Asn, and the $C^{\delta}O$ carbons of Glu and Gln) and the adjacent CH_2 protons (the $C^{\beta}H$ protons of Asp and Asn, and the $C^{\gamma}H$ protons of Glu and Gln). In the spectrum, additional cross peaks between the backbone carbonyl carbon resonance and the $C^{\alpha}H$ proton resonance are observed. Because the $C^{\alpha}H$ proton resonances appeared at low field away from the CH_2 protons, the additional cross peaks were clearly distinguishable from the concerned peaks, although they provide important information about the backbone conformation and the ionization state of the C-terminal carboxyl group.

The pH-dependent chemical shifts of the carboxyl carbon resonances for all of the carboxyl groups in *E. coli* RNase HI are shown in Figure 2. The titration shifts were analyzed by nonlinear least-squares curve fitting, and the determined pK_a values are listed in Table 1. The following residues, Asp10, Asp70, Asp102, Asp108, Asp148, Glu32, Glu57, and Glu129, showed significant shifts of over 0.7 pH unit from their normal pK_a values.

Most of the titration curves have simple sigmoidal shapes, between the ionized (deprotonated) and the neutral (protonated) states of the carboxyl group, except for Asp10, -70, -102, and -148. For Asp10 and Asp70, two-step titrations are observed around pH 2.5 and 6.5. For Asp102 and Asp148, the carboxyl groups were not titrated in the pH range from 2 to 8. Indeed, the chemical shift of Asp148 does not change at all in the pH range. The carboxyl carbons for the other residues appear between 176 and 179 ppm in the deprotonated state and between 173 and 175 ppm in the protonated state. The carboxyl carbon of Asp148 resonates at 177.6 ppm, thus indicating that Asp148 is in the deprotonated state and its pK_a value is below 2. This assignment is also compatible with a remarkable salt bridge with Arg46 in the neighborhood of Asp102 and Asp148 in the X-ray crystal structure (Katayanagi *et al.*, 1992), as discussed below.

The pH-dependent chemical shifts of the adjacent CH proton resonances are shown in Figure 3, and the determined pK_a values are listed in Table 1. Contrary to the case of the carboxyl carbon resonances, most of the titration curves are not simply sigmoidal, although the $pK_a^{1/2}$ values are not far from the associated ones determined from the carboxyl carbon resonances. This complication may arise from the susceptibility of the proton chemical shift to other factors and reveals a drawback of its use for pH titration.

The backbone conformational changes were monitored during the pH titration by observing the chemical shift changes of the backbone carbonyl carbon and the $C^{\alpha}H$ proton resonances. The observed chemical shifts of the backbone resonances were highly dispersed, from 2.5 to 6.0 ppm for ^1H and 167 to 180 ppm for ^{13}C, in all of the spectra, and their chemical shift changes, except for the C-terminal α-carboxylate of Val155, were less than 0.5 ppm for ^1H and 2 ppm for ^{13}C during the pH titration. This suggests that large structural changes do not occur in the global fold of the protein in the pH range from 2 to 8.

Determination of the pK_a Values in the Presence of Mg^{2+} Ion. The pK_a values of the carboxyl groups in the presence of Mg^{2+} ion were determined in the same manner as described above. Each titration curve, except for Asp10 and Asp70, has a simple sigmoidal shape, as shown in Figure 4. For Asp10 and Asp70, two-step titrations similar to those for the free enzyme were observed. The determined pK_a values are listed in Table 1. The remarkable pK_a change in the presence of Mg^{2+} ion was only observed for Asp10. The pK_a values of the other residues were well conserved.

The Mg^{2+} ion concentration (150 mM; 100 equiv to the enzyme) used in the pH titration experiment was chosen by referring to the saturation curves of Mg^{2+} ion binding to the enzyme at pH 5.5. The saturation curves were obtained from

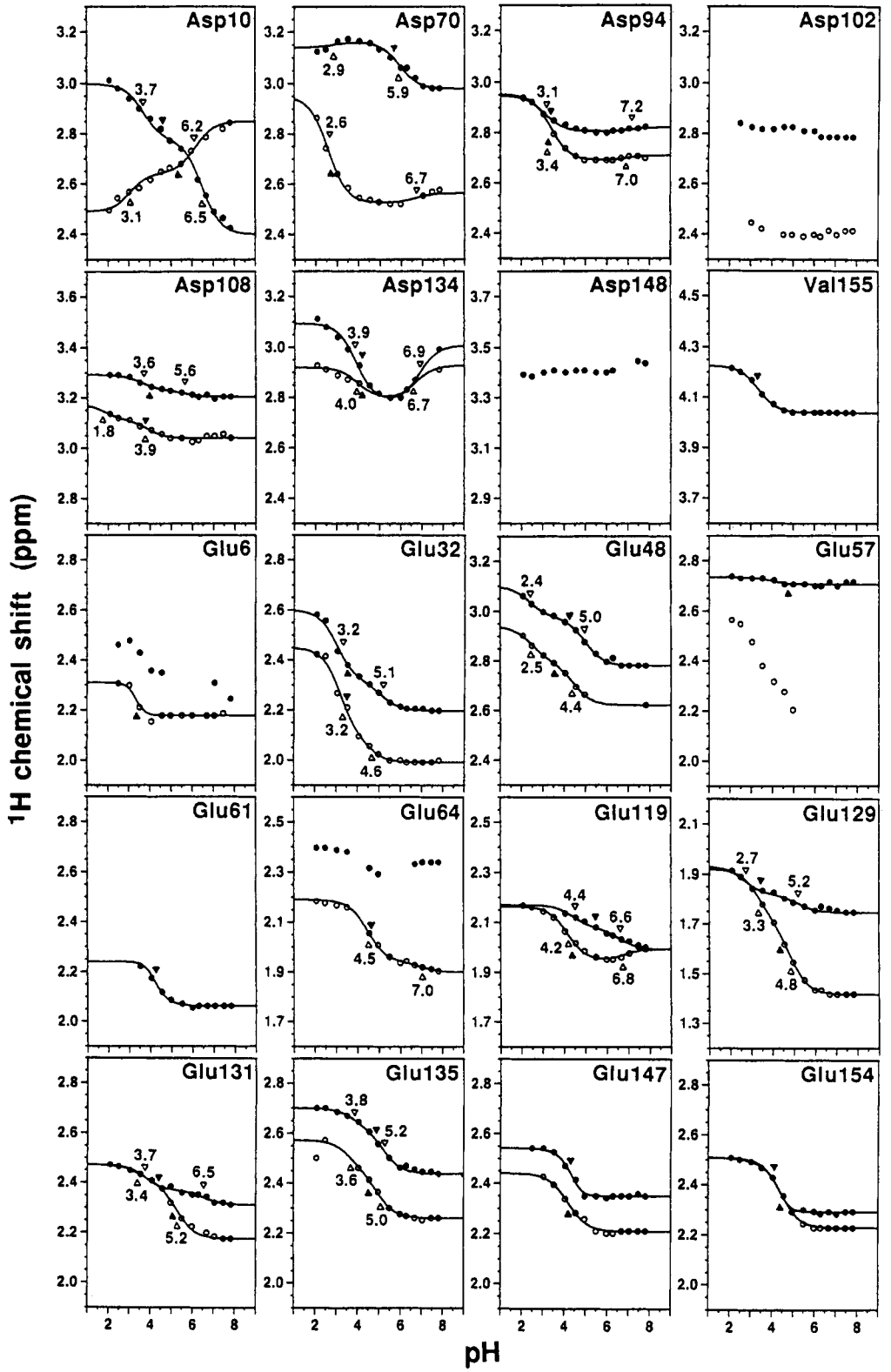

FIGURE 3: pH dependence of the chemical shifts of the adjacent proton resonances to carboxyl groups in *E. coli* RNase HI. Each of the two methylene protons (the $C^{\beta}H$ protons of Asp and the $C^{\gamma}H$ protons of Glu) is denoted by closed and open circles, respectively. For Glu61, the chemical shifts of the two methylene protons are degenerate. For Asp148, one of the proton resonances was lost due to peak broadening. The fitted titration curves are shown by solid lines. For Glu6, Glu57, and Glu64, one of the titration shifts could not be fitted due to insufficient data. The pK_a^{app} values (open triangles) and the $pK_a^{1/2}$ values (closed triangles) are also shown. The experiments are the same as in Figure 2.

the Mg^{2+}-titration experiment, in which the chemical shift changes of the carboxyl carbon resonances were observed in the 2D $^{13}C'$–(^{13}C)–^{1}H HSQC/HSQC spectra. The variations $\Delta\delta$ of the chemical shifts with the addition of 150 mM $MgCl_2$ at pH 5.5 are shown in the right column of Table 1. Significant changes (above 0.3 ppm) in the chemical shifts with the Mg^{2+} ion binding were observed for the carboxyl groups of Asp10, Glu48, Asp70, Glu131, Asp134, and Glu135. The titration curves of these residues are fairly saturated at a concentration of 150 mM $MgCl_2$ at pH 5.5. We have already reported that a single Mg^{2+} ion binds with a weak binding constant (K_D is 4 mM at pH 5.5 from the Hill plot) to the active site of the

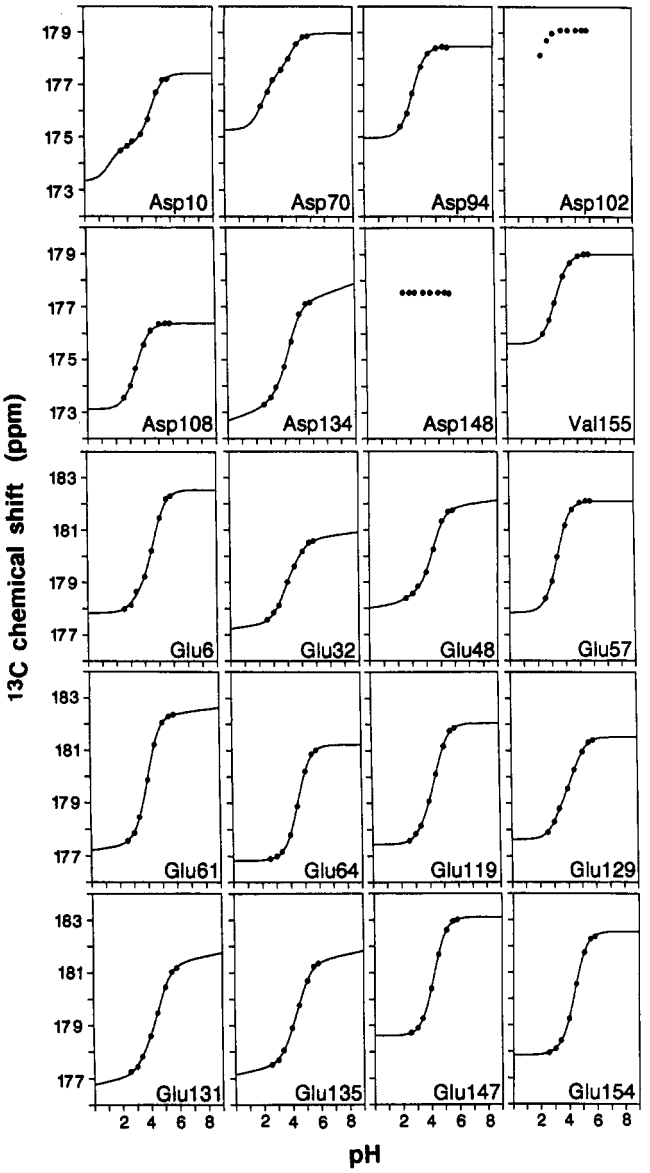

FIGURE 4: pH dependence of the chemical shifts of the carboxyl carbon resonances for all of the carboxyl groups in *E. coli* RNase HI, in the presence of 150 mM $MgCl_2$. The fitted titration curves are also shown by solid lines.

enzyme, as determined by the change in chemical shift of the backbone amide resonances using ^1H–^{15}N heteronuclear NMR (Oda *et al.*, 1991). The results shown in this report are consistent with the previous results.

Theoretical Calculation of the pK_a Values of the Carboxyl Groups. The pK_a values of the carboxyl groups in *E. coli* RNase HI were theoretically calculated as mentioned. Asp102 and Asp148 are well separated from the other carboxylates, and the electrostatic potential at the two carboxyl groups was highly positive due to the interactions from all the basic residues and the backbone peptides. In fact, the $pK_a^{1/2}$ values of the two carboxylates were calculated as highly negative (–5.0 and –7.7, respectively), when all the other carboxyl groups were assumed to have their normal pK_a values. Therefore, when combined in the partition function calculation, the carboxylates of the two residues were always assumed to be fully ionized. The calculated pK_a values for all the other residues are listed in Table 2. The experimentally observed pK_a shifts are satisfactorily reproduced by the calculation. The $pK_a^{1/2}$ values calculated with a dielectric constant (ϵ_p) of 10 in the protein interior fit better with the observed $pK_a^{1/2}$ values than those with $\epsilon_p = 4$. The calculated pH titration curves of Asp10 and Asp70 with $\epsilon_p = 10$ are shown in Figure 5B. The two-step titrations observed in the experimental curves in Figure 5A are well reproduced, especially for Asp10.

Table 2: Calculated Values for the Ionization Constant (pK_a), the Solvent Accessibility (ASA), and the Mobility (*B* Factor) of Carboxyl Groups in *E. coli* RNase HI

residue	$pK_a^{1/2}$ [a] ($\epsilon_p = 4$)	$pK_a^{1/2}$ [a] ($\epsilon_p = 10$)	ASA[b] (Å^2)	*B* factor[c] (Å^2)
Asp10	5.4 (5.8/0.2)	5.4 (5.9/1.1)	17.9	16.5
Asp70	2.1	2.8	32.4	20.8
Asp94	1.7	2.4	73.7	27.9
Asp102	–[d]	–[d]	41.1	14.9
Asp108	1.6	2.0	33.3	20.0
Asp134	2.7	3.0	50.0	21.3
Asp148	–[d]	–[d]	1.9	15.3
Glu6	2.2	2.8	34.2	18.4
Glu32	1.7	2.4	55.2	28.7
Glu48	2.8	3.3	17.8	21.2
Gly57	2.4	2.8	54.3	15.1
Glu61	2.4	2.7	66.8	35.1
Glu64	3.9	3.9	82.4	26.0
Glu119	2.6	2.8	52.3	26.6
Glu129	–0.7	0.8	27.8	22.5
Glu131	4.6	4.5	103.2	26.1
Glu135	4.2	4.2	105.0	24.9
Glu147	4.4	4.4	119.4	29.2
Glu154	1.4	2.9	81.7	54.3
Val155	2.8	2.7	55.6	53.4

[a] The numbers in parentheses refer to the pK_a^{app} values, defined as the apparent macroscopic ionization constants by Shrager *et al.* (1972). [b] The values of the accessible surface area (ASA) for side-chain atoms were calculated from the X-ray structure by Katayanagi *et al.* (1992), following the calculation method of Ooi and Oobatake (1988). [c] The values of average isotropic temperature factors (*B* factors) for side-chain atoms were obtained from the data of the crystal structure determined by Katayanagi *et al.* (1992). [d] These residues were always considered to be ionized (see the text).

The calculated pK_a values fairly match the experimental ones, but not completely, because of several approximations made in the calculation, as discussed by Takahashi *et al.* (1992): (1) the protein structure is fixed to one conformation, (2) the distribution of dielectric constants is simplified to be homogeneous in the three regions, the inside, interface, and outside of the protein molecule, and (3) the self-energy term, which is very sensitive to the dielectric constant, is disregarded. Nevertheless, they provide crucial information for the interpretation of the experimental results and for the consideration of the underlying molecular mechanism of the titration shifts.

DISCUSSION

pH Titration by $^{13}C'$–(^{13}C)–^1H HSQC/HSQC Experiments. The sensitivity of the NMR experiment is crucial to fix precise ionization constants by pH titration. The $^{13}C'$–(^{13}C)–^1H HSQC/HSQC experiment using the proton detection of ^{13}C resonances through the large *J* couplings ($^1J_{C-H}$ = 140 Hz and $^1J_{C-C}$ = 30–40 Hz) is quite appropriate for this study due to its high sensitivity.

With this technique, the ionization states of the carboxyl groups can be investigated by both the chemical shift changes of the carbon resonances and the adjacent CH proton resonances. For Glu147, which has the most exposed side-chain carboxyl group in the protein, both titration curves show simple sigmoidal shapes as shown in Figures 2 and 3. However, complications are often observed in the proton resonance titration curves (Figure 3) as compared to those of the carbon resonance titration curves (Figure 2). For Glu119, for example, the carbon resonance titration curve shows a simple

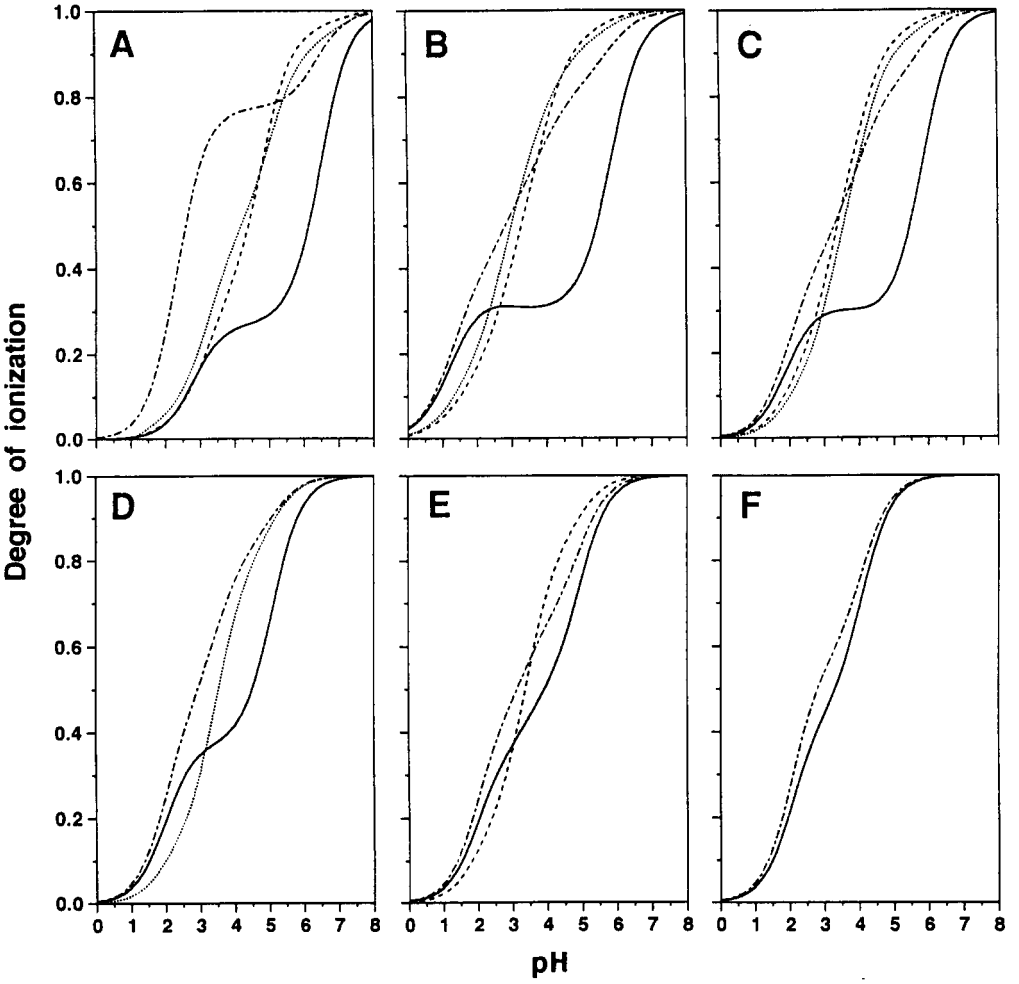

FIGURE 5: Normalized pH titration curves of the catalytic Asp10 (solid line), Asp70 (dashed-and-dotted line), Asp134 (dotted line), and Glu48 (dashed line): (A) experimental titration curve of the free enzyme; (B) theoretically calculated curve with the ϵ_p of 10 of the free enzyme. (C) Calculated titration curve, only considering the ionization of four groups, Asp10, Asp70, Asp134, and Glu48. Other residues were assumed to be completely ionized. (D) Same as panel C, but the ionizations of only Asp10, Asp70, and Asp134 were considered. (E) Only the ionizations of Asp10, Asp70, and Glu48 were considered. (F) Only the ionizations of Asp10 and Asp70 were considered.

sigmoidal shape, but the proton resonance titration curves show a two-step change. The interpretation of the curves of the two methylene protons is also quite difficult, because they behave very differently. This phenomenon may be attributable to the indirect effects of the chemical shift changes other than the ionization itself. The intrinsic ionization state of the concerned carboxyl group seems to be reflected better in the chemical shift of the carboxyl carbon resonances than in that of the proton resonances. Thus, we adopted the pK_a values determined from the ^{13}C data to discuss the ionization states of the carboxyl groups in *E. coli* RNase HI.

pK_as of the Catalytic Residues. Asp10 and Asp70 are essential for the catalytic activity, together with Glu48 (Kanaya *et al.*, 1990). The present result reveals that the carboxyl groups of Asp10 and Asp70 have unusual pK_a values. The p$K_a^{1/2}$ of Asp10 (6.1) is abnormally high, and that of Asp70 (2.6) is very low. The carboxyl groups of the two Asp residues are located close to each other in the crystal structure (Figure 6), leading to a strong interaction between them.

This situation is similar to that of the two catalytic Asp residues, Asp32 and Asp215, in pepsin-like aspartic proteases (Hsu *et al.*, 1977; Blundell *et al.*, 1985). The ionization of the carboxyl pair in pepsin was explained by comparing it to the ionization of maleic acid. Maleic acid, which is a dicarboxyl compound, has pK_as of 1.9 and 6.3, due to the intramolecular interaction between the two carboxyl groups. This special property of the ionization observed for maleic acid is known to be a general property in dicarboxyl compounds. In hen egg-white lysozyme, an unusual ionization behavior has been observed for the catalytic carboxylates of Glu35 and Asp52 (Parsons & Raftery, 1972a). It seems that the ionization behavior and the mechanism of the catalytic carboxyl pair are essentially the same between aspartic proteases, lysozyme, and *E. coli* RNase HI.

The strong interaction and cooperative action between Asp10 and 70 are experimentally confirmed by the remarkable two-step titration curves seen in Figure 5A. In proton NMR observations, these complex titration curves were often interpreted as the electric field effect on the chemical shift, due to the ionization of the neighboring residues. However, in the current experiment, the comparison between the theoretical and experimental results unambiguously revealed the direct effect of the electrostatic interaction, which leads to the change of ionization states at the two carboxyl groups. In fact, the two-step titrations are reproduced by the theoretical calculation, especially well for Asp10, as shown in Figure 5B. For residues involved in strong mutual electrostatic interactions, cooperative behaviors have been generally predicted (Bashford & Gerwert, 1992; Yang *et al.*, 1993).

In order to analyze the cooperative action, the pH titration curves of Asp10 and -70 were calculated by considering the ionization states of only two other residues in their neighbor-

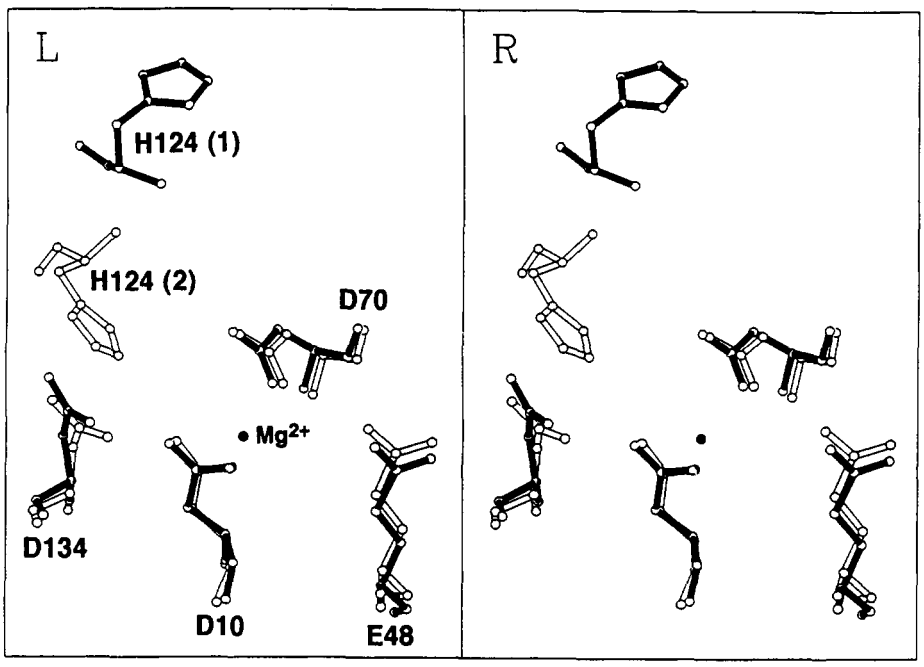

FIGURE 6: Stereoview of the structure around the active site in *E. coli* RNase HI. Side chains of active site residues (Asp10, Glu48, and Asp70), as well as those of well conserved residues (His124 and Asp134) in the crystal structure of Katayanagi *et al.* (black lines), were superimposed upon those in the crystal structure of Yang *et al.* (white lines). The position of the Mg^{2+}, as determined by the crystal soaking method (Katayanagi *et al.*, 1992) is also shown (black dot). The active site residues are very similar in the two crystal structures except His124, which takes two different positions. The pH conditions were almost the same (pH 8.8–9.0) in the two crystals. The structures of Katayanagi *et al.* and Yang *et al.* are deposited in the Protein Data Bank as 2RN2 and 1RNH, respectively.

hood, Glu48 and Asp134. In this artificial case, all the other carboxylates and His residues were assumed to be ionized, except for the neutral His114. The results are shown in Figure 5C, and they are very similar to those obtained when all the carboxyl groups are considered (Figure 5B). This means that the two-step titrations of Asp10 and -70 can mainly be explained by the cooperative ionization of these four carboxyl groups. From a further analysis considering only the ionization of Asp10, -70, and -134, a remarkable two-step titration of Asp10 was also observed (Figure 5D). In contrast, when only Asp10 and -70 and Glu48 were considered, the anomalous titration curves of Asp10 and -70 were not reproduced, as in Figure 5E. These are similar to those in Figure 5F, where only Asp10 and Asp70 were considered. The result strengthened the conclusion that the two-step titration of Asp10 is profoundly governed by the interaction among the three residues, Asp10, -70, and -134. The strongest electrostatic interaction is between Asp10 and -70, and the interaction between Asp70 and -134 is about 60% weaker than that between Asp10 and -134, as revealed from the numerical calculation. Therefore, below pH 2, both Asp10 and -70 begin to ionize in a similar manner. Above pH 2, the ionization process of Asp134 holds the further ionization of Asp10 to approximately 30% until pH 4.5, where Asp70 and -134 almost finish their ionizations. Glu48 contributes little to the two-step titration, probably because it has a similar extent of electrostatic interaction with Asp10 and with Asp70.

The above analysis is based upon a static macroscopic model of the protein solution, considering only a through space electrostatic interaction. In contrast, this cooperative phenomenon can also be explained in a microscopic view by a putative intramolecular hydrogen bonding interaction (Perrin & Thoburn, 1992), in which the remaining proton is shared by both carboxylate groups of Asp10 and Asp70. This carboxylate–carboxylic acid interaction can stabilize the protonated Asp10 even at higher pH than the normal pK_a value of an Asp residue.

The titration curve of Glu48 was typically sigmoidal, and the pK_a shift from the normal value was small, although Glu48 is in the active site and its carboxyl group stays very close to Asp10 and -70, as shown in Figure 6. Since the degree of ionization of Asp10 is less than 30% below pH 4.5, the electrostatic effects from the two carboxylates are not as large as in the situation with two completely negative charges in the neighborhood. In fact, the calculated titration curve of Glu48 was sigmoidal and the pK_a shift was not as large.

In the presence of Mg^{2+} ion, the pK_a values of the carboxylates involved in the Mg^{2+} binding are determined by competitive binding with the proton and the Mg^{2+} ion. The influence of the competition was observed only in the titration shift of Asp10. The pK_a value of Asp10 changed from 6.5 to 4.7 in the presence of the Mg^{2+} ion. We have previously reported that the binding affinity of the metal ion to *E. coli* RNase HI is rather weak (K_D = 4 mM) at pH 5.5 (Oda *et al.*, 1991). That weak binding constant at pH 5.5 may be due to the competition with the protonation of the Asp10 carboxylate.

pK_as of the Other Asp Residues and Structural Influence. Asp94 lies in the Lys- and Arg-rich loop following the third helix, and the electrostatic potential environment of this region is strongly positive (Katayanagi *et al.*, 1990; Yang *et al.*, 1990). Therefore, the positive electrostatic environment around the residue should contribute considerably to the downward pK_a shift of Asp94. This is supported by the reproduced pK_a shift in the calculation. Asp94 interacts with Thr92 in the crystal, so the observed pK_a shift of Asp94 may be caused partly by this interaction.

Asp148 is the most deeply buried acidic residue in the protein. In the crystal, this Asp residue interacts with Arg46, which is the only basic residue pointing forward the inside of the molecule. Asp102 also forms a salt bridge with Arg46, which creates an ionic interaction network. The *B* factors of the two residues are also very low, as shown in Table 2. The unusual low pK_as of Asp102 and Asp148 can be explained by

the strong electrostatic interaction network.

Asp108 makes a salt bridge with Lys86 in the crystal. The downward shift observed for the pK_a of Asp108 can be explained by this interaction.

Asp134 interacts with Arg138 in the crystal, which causes a downward pK_a shift for Asp134. However, the determined pK_a value of Asp134 is near the normal value. One simple explanation is that the side-chain carboxyl of Asp134 is flexible and the interaction between Asp134 and Arg138 is rather weak in the solution. On the other hand, the ionization of Asp134 is affected by the active site carboxylates, as previously discussed. The negative charges of these carboxyl groups will cause an upward pK_a shift in Asp134. Therefore, the determined normal pK_a value of Asp134 is interpreted as the result of a combination of two opposing effects.

pK_as of Other Carboxyl Groups and Structural Influence. The pK_a values for the Glu64, Glu131, Glu135, Glu147, and Glu154 residues are close to the normal pK_a value, implying that these carboxyl groups are not buried in the protein and do not exert strong electrostatic interactions. This is consistent with the results of the crystal structural analysis. These residues are flexible and well exposed to the solvent, as shown by the ASA and *B* factor values in Table 2.

Glu57 interacts with Arg106 in the crystal. The downward shift observed for the pK_a of Glu57 can be explained by this interaction.

The carboxyl groups of Glu6, Glu32, and Glu129 are involved in an electrostatic interaction network with the guanidino group of Arg27 inside the protein in the crystal. The downward shifts of the pK_a values of Glu32 and Glu129 can be explained by this interaction. In contrast, the observed pK_a value of Glu6 is almost normal, for unkown reasons. A simple explanation for this would be that the side-chain carboxyl group is out of the network in the solution structure, and the interaction between Glu6 and Arg27 is weak.

For the other two residues, Glu61, and Glu119, the pK_a shifts were not so large. This implies simply that these carboxyl groups are not involved in a strong electrostatic interaction. The crystal structural analysis suggests that these residues do not interact with the strongly basic amino acids, Lys and Arg; Glu61 interacts with Tyr28, and Glu119 interacts with Ser68 and His127.

The C-terminal α-carboxylate of Val155 has the normal pK_a value, because it is very flexible and exposed to the solvent.

Catalytic Mechanism of RNase H. It has been reported that the optimal pH for the catalytic reaction of *E. coli* RNase HI is 8 (Berkower *et al.*, 1973). The pK_a corresponding to this pH is not found either in the carboxyl groups of the Mg^{2+}-free or the Mg^{2+}-bound enzyme or in the His residues, the pK_a values of which were previously determined in the free enzyme (Oda *et al.*, 1993). The ionized water molecule, which is thought to attack the phosphodiester bond of the RNA, may directly associate at the optimal pH.

In the carboxylate–hydroxyl relay mechanism proposed by our group (Nakamura *et al.*, 1991), three carboxylates have to be involved in the catalytic action. One of them acts as a general base, which abstracts the proton from a water molecule to release a hydroxyl ion that subsequently nucleophilically attacks the phosphate group. The other carboxylate acts as a general acid, which donates the proton to the leaving O3′ of the RNA strand. The last one binds the metal ion, which stabilizes the transition state and correctly positions the phosphate group relative to the enzyme. Since Asp10 with its high pK_a maintains a protonated state at a higher pH than any other carboxylate, Asp10 could be the proton donor in the catalytic reaction. The unusually low pK_a of Asp70 suggests that its carboxyl group can act as a general base. Therefore, Asp70 should be considered as the residue that activates the water molecule. Alternatively, the role of Glu48 could be in Mg^{2+} ion binding. The interpretations for the roles of Glu48 and Asp70 are confirmed by the crystal structure of the Mg^{2+}-bound enzyme, in which the Mg^{2+} ion lies within a distance suitable for coordination with the carboxyl group of Glu48, but not with Asp70 (Katayanagi *et al.*, 1992, 1993).

Although Asp10 is likely to act as a proton donor in the catalytic reaction, the pH titration curve of Asp10 suggests that its carboxyl group favors the deprotonated form at the optimal pH of 8. Furthermore, when Mg^{2+} ion binds to the enzyme, the pK_a of Asp10 is shifted to a lower value. The carboxyl group of Asp10 is likely to be involved in the interaction with the metal ion, as shown by the crystal structural analysis (Katayanagi *et al.*, 1990, 1992, 1993; Davies *et al.*, 1991). In the present results, the largest changes in the ^{13}C chemical shift and the pK_a value upon the Mg^{2+} ion binding were observed only as Asp10, among all the carboxyl groups, suggesting that Asp10 directly binds the Mg^{2+} ion.

These results seem to contradict the role of Asp10 proposed in the carboxylate–hydroxyl relay model. If the role of Asp10 must be revised from proton donor to metal ion binding, we have to find another candidate for the proton donor. His124 is one of the well conserved residues among the RNase H family (Doolittle *et al.*, 1989), and it may be able to act as a proton donor in the revised mechanism, although its replacement by other amino acids did not completely abolish the enzymatic activity (Oda *et al.*, 1993). For His124, another role as a "proton shuttle" for the general base (Asp70) has been proposed on the basis of the original carboxylate–hydroxyl relay model (Oda *et al.*, 1993).

To reveal the catalytic mechanism of the enzyme, we should consider the ionization states of the carboxyl groups in the active site for the complex of the negative charged substrate, the DNA/RNA hybrid, and the enzyme. In hen egg-white lysozyme, it has been reported that the pK_a of the catalytic Glu35 exhibits a basic shift (to a pK_a above 8) upon substrate binding (Parsons & Raftery, 1972b). Active-site pK_a shifts due to substrate binding have also been observed for the aspartic proteases (Lin *et al.*, 1992). Unfortunately, it is presently not feasible to determine the pK_as of *E. coli* RNase HI in complex with a substrate and a divalent metal ion, because the substrate is cleaved immediately due to the catalytic reaction and a large amount of precipitate is formed (Nakamura *et al.*, 1991).

CONCLUSION

The carboxyl carbon resonances observed in the current study are very reliable reporters for studies of the ionization states and pK_as of the individual carboxyl groups in proteins at various pH values. The multistep titration curves can be interpreted with the aid of theoretical calculations based upon the continuum model.

It is shown that the pK_as of carboxyl groups are highly perturbed in the enzyme. The pK_a shifts are caused by microscopic and macroscopic electrostatic effects. Most of the downward pK_a shifts are explained by direct electrostatic interactions with the neighboring groups. The catalytic residues of Asp10 and 70 have unusual pK_a values ($pK_a^{1/2}$ 6.1 and 2.6, respectively) with significant two-step titrations, which are produced by the strong electrostatic interactions among the four carboxylates in the active site. The protonation states of these carboxylates should govern the catalysis of the enzyme,

as observed in lysozyme and aspartic protease. The current study provides more refined insight into the enzymatic activity and especially the role of the carboxyl group of each of the catalytic residues. Asp10 could donate a proton as a general acid, or it may directly bind the Mg^{2+} ion. Asp 70 activates a water molecule as a general base.

ACKNOWLEDGMENT

We thank Dr. T. Ohkubo for help in NMR measurements, Dr. M. Oobatake for help in the calculation of ASA values, and Drs. K. Morikawa, K. Katayanagi, and M. Yoshida for helpful discussions.

REFERENCES

Arnold, E., Jacobo-Molina, A., Nanni, R. G., Williams, R. L., Lu, X., Ding, J., Clark Jr., A. D., Zhang, A., Ferris, A. L., Clark, P., Hizi, A., & Hughes, S. H. (1992) *Nature 357*, 85–89.

Bashford, D., & Karplus, M. (1990) *Biochemistry 29*, 10219–10225.

Bashford, D., & Karplus, M. (1991) *J. Phys. Chem. 95*, 9556–9561.

Bashford, D., & Gerwert, K. (1992) *J. Mol. Biol. 224*, 473–486.

Bashford, D., Case, D. A., Dalvit, C., Tennant, L., & Wright, P. E. (1993) *Biochemistry 32*, 8045–8056.

Berkower, I., Leis, J., & Hurwitz, J. (1973) *J. Biol. Chem. 248*, 5914–5921.

Blundell, T., Jenkins, J., Pearl, L., Sewell, T., & Pedersen, V. (1985) in *Aspartic Proteinases and Their Inhibitors* (Kostka, V., Ed.) pp 151–161, Walter de Gruyter, Berlin.

Crouch, R. J. (1990) *New Biol. 2*, 771–777.

Crouch, R. J., & Dirksen, M.-L. (1982) in *Nuclease* (Linn, S. M., & Roberts, R. J., Eds.) pp. 211–241, Cold Spring Harbor Laboratory, Cold Spring Harbor, NY.

Davies, J. F., II, Hostomska, Z., Hostomsky, Z., Jordan, S. R., & Matthews, D. (1991) *Science 252*, 88–95.

Doolittle, R. F., Feng, D.-F., Johnson, M. S., & McClure, M. A. (1989) *Q. Rev. Biol. 64*, 1–30.

Fersht, A. (1985) in *Enzyme Structure and Mechanism*, pp 156, W. H. Freeman, New York.

Hol, W. G. J., van Duijnen, P. T., & Berendsen, H. J. C. (1978) *Nature 273*, 443–446.

Hsu, I.-N., Delbaere, L. T. J., James, M. N. G., & Hofmann, T. (1977) *Nature 266*, 140–145.

Ishikawa, K., Okumura, M., Katayanagi, K., Kimura, S., Kanaya, S., Nakamura, H., & Morikawa, K. (1993) *J. Mol. Biol. 230*, 529–542.

Jardetzky, O., & Roberts, G. C. K. (1981) in *NMR in Molecular Biology*, pp 281–284, Academic Press, New York.

Jou, R., & Cowan, J. A. (1991) *J. Am. Chem. Soc. 113*, 6685–6686.

Kanaya, S., & Crouch, R. J. (1983) *J. Biol. Chem. 258*, 1276–1281.

Kanaya, S., Kohara, A., Miyagawa, M., Matsuzaki, T., Morikawa, K., & Ikehara, M. (1989) *J. Biol. Chem. 264*, 11546–11549.

Kanaya, S., Kohara, A., Miura, Y., Sekiguchi, A., Iwai, S., Inoue, H., Ohtsuka, E., & Ikehara, M. (1990) *J. Biol. Chem. 265*, 4615–4621.

Kanaya, S., Katsuda, C., Kimura, S., Nakai, T., Kitakuni, E., Nakamura, H., Katayanagi, K., Morikawa, K., & Ikehara, M. (1991a) *J. Biol. Chem. 266*, 6038–6044.

Kanaya, S., Katsuda, C., & Ikehara, M. (1991b) *J. Biol. Chem. 266*, 11621–11627.

Kanaya, S., Katayanagi, K., Morikawa, K., Inoue, H., Ohtsuka, E., & Ikehara, M. (1991c) *Eur. J. Biochem. 198*, 437–440.

Kanaya, S., Oobatake, M., Nakamura, H., & Ikehara, M. (1993) *J. Biotechnol. 28*, 117–136.

Katayanagi, K., Miyagawa, M., Matsushima, M., Ishikawa, M., Kanaya, S., Ikehara, M., Matsuzaki, T., & Morikawa, K. (1990) *Nature 347*, 306–309.

Katayanagi, K., Miyagawa, M., Matsushima, M., Ishikawa, M., Kanaya, S., Nakamura, H., Ikehara, M., Matsuzaki, T., & Morikawa, K. (1992) *J. Mol. Biol. 223*, 1029–1052.

Katayanagi, K., Okumura, M., & Morikawa, K. (1993) *Proteins: Struct., Funct., Genet. 17*, 337–346.

Kohda, D., Sawada, T., & Inagaki, F. (1991) *Biochemistry 30*, 4896–4900.

Kohlstaedt, L. A., Wang, J., Friedman, J. M., Rice, P. A., & Steitz, T. A. (1992) *Science 256*, 1783–1790.

Lin, Y., Fusek, M., Lin, X., Hartsuck, J. A., Kezdy, F. J., & Tang, J. (1992) *J. Biol. Chem. 267*, 18413–18418.

Linderstrøm-Lang, K. (1924) *C. R. Trav. Lab. Carlsberg 15*, 1–29.

Nagayama, K., Yamazaki, T., Yoshida, M., Kanaya, S., & Nakamura, H. (1990) *J. Biochem. (Tokyo) 108*, 149–152.

Nakamura, H. (1988) *J. Phys. Soc. Jpn. 57*, 3702–3705.

Nakamura, H., & Nishida, S. (1987) *J. Phys. Soc. Jpn. 56*, 1609–1622.

Nakamura, H., Sakamoto, T., & Wada, A. (1989) *Protein Eng. 2*, 177–183.

Nakamura, H., Oda, Y., Iwai, S., Inoue, H., Ohtsuka, E., Kanaya, S., Kimura, S., Katsuda, C., Katayanagi, K., Morikawa, K., Miyashiro, H., & Ikehara, M. (1991) *Proc. Natl. Acad. Sci. U.S.A. 88*, 11535–11539.

Oda, Y., Nakamura, H., Kanaya, S., & Ikehara, M. (1991) *J. Biomol. NMR 1*, 247–255.

Oda, Y., Nakamura, H., Yamazaki, T., Nagayama, K., Yoshida, M., Kanaya, S., & Ikehara, M. (1992) *J. Biomol. NMR 2*, 137–147.

Oda, Y., Yoshida, M., & Kanaya, S. (1993) *J. Biol. Chem. 268*, 88–92.

Ooi, T., & Oobatake, M. (1988) *J. Biochem. (Tokyo) 104*, 440–444.

Parsons, S. M., & Raftery, M. A. (1972a) *Biochemistry 11*, 1623–1629.

Parsons, S. M., & Raftery, M. A. (1972b) *Biochemistry 11*, 1633–1638.

Perrin, C. L., & Thoburn, J. D. (1992) *J. Am. Chem. Soc. 114*, 8559–8565.

Richarz, R., & Wüthrich, K. (1978) *Biochemistry 17*, 2263–2269.

Sakamoto, T., Nakamura, H., Uedaira, H., & Wada, A. (1989) *J. Phys. Chem. 93*, 357–366.

Shrager, R. I., Cohen, J. S., Heller, S. R., Sachs, D. H., & Schechter, A. N. (1972) *Biochemistry 11*, 541–547.

Takahashi, S., & Nagayama, K. (1988) *J. Magn. Reson. 76*, 347–351.

Takahashi, T., Nakamura, H., & Wada, A. (1992) *Biopolymers 32*, 897–909.

Tanford, C., & Roxby, R. (1972) *Biochemistry 11*, 2129–2198.

Warwicker, J., & Watson, H. C. (1982) *J. Mol. Biol. 157*, 671–679.

Wintersberger, U. (1990) *Pharmacol. Ther. 48*, 259–280.

Yamazaki, T., Yoshida, M., Kanaya, S., Nakamura, H., & Nagayama, K. (1991) *Biochemistry 30*, 6036–6047.

Yamazaki, T., Yoshida, M., & Nagayama, K. (1993) *Biochemistry 32*, 5656–5669.

Yang, A.-S., Gunner, M. R., Sampogna, R., Sharp, K., & Honig, B. (1993) *Proteins: Struct., Funct., Genet. 15*, 252–265.

Yang, W., Hendrickson, W. A., Crouch, R. J., & Satow, Y. (1990) *Science 249*, 1398–1405.